33rd Annual International Conference of the IEEE EMBS
Boston, Massachusetts USA, August 30 - September 3, 2011

Detection of Ventricular Suction in an Implantable Rotary Blood Pump Using Support Vector Machines

Yu Wang, George Faragallah, Eduardo Divo, and Marwan A. Simaan, *Fellow, IEEE*

***Abstract*—A new suction detection algorithm for rotary Left Ventricular Assist Devices (LVAD) is presented. The algorithm is based on a Lagrangian Support Vector Machine (LSVM) model. Six suction indices are derived from the LVAD pump flow signal and form the inputs to the LSVM classifier. The LSVM classifier is trained and tested to classify pump flow patterns into three states: No Suction, Approaching Suction, and Suction. The proposed algorithm has been tested using existing in vivo data. When compared to three existing methods, the proposed algorithm produced superior performance in terms of classification accuracy, stability, and learning speed. The ability of the algorithm to detect suction provides a reliable platform in the development of a pump speed controller that has the capability of avoiding suction.**

I. Introduction

IN recent years, the rotary Left Ventricular Assist Device (LVAD) has been successfully used as a mechanical support device for many patients suffering from congestive heart failure. The rotary LVAD is a mechanical pump surgically implanted from the left ventricle to the aorta to help maintain the flow of blood from the patient's heart, which cannot effectively work on its own. In order to meet the circulatory demand of the patient, developing an appropriate pump control system to adjust the blood flow through the pump by controlling the rotational speed of the pump is an important challenge facing the increased use of these devices.

An important constraint that should be taken into consideration is to insure that the pump is rotated at a speed below a threshold beyond which the pump attempts to draw more blood from the left ventricle than available causing a phenomenon called ventricular suction. This phenomenon, which could cause collapse of the ventricle, is dangerous and needs to be detected and corrected by lowering the pump speed.

Several approaches have been used to detect suction. Among these are ones that extract features from the pump flow signal (which is one of very few signals that can be easily measured) and use powerful pattern recognition algorithms to classify the signal into different states and detect suction. These classifiers vary from simple threshold comparisons [1] to more complex techniques such as Classification and Regression Tree (CART) [2], Discriminant Analysis (DA) [3], and Neural Networks (NN) [4].

In this paper, we introduce a new suction detection and classification algorithm based on the Lagrangian Support Vector Machine (LSVM) method in pattern recognition. The LSVM is a modified standard Support Vector Machine (SVM) and has high accuracy, stable performance, and fast learning speed. Several real-time applications of the SVM method in different fields have been reported in the literature [5], [6]. The paper is organized as follows. Section II describes the proposed classification strategy in details. Section III shows the experimental results of the proposed algorithm. Section IV compares these results to three existing approaches and discusses the feasibility of real-time application of the proposed method. Concluding remarks are presented in Section V.

II. Pump Status and Suction Indices

A. Definition of Pump Status

Fig. 1 shows the flow chart of the proposed algorithm. The feature extraction module calculates six indices from the processed pump flow, which allow determination of pump status. In this research, the pump status can be defined as follows:

1) No Suction (NS): This corresponds to the normal operating condition of the pump. Within each cardiac cycle, the Minimum Pump Inlet Pressure (MPIP) is generally close to zero and its difference from the Minimum Left Ventricular Pressure (MLVP) is small (i.e., $\Delta P = MLVP - MPIP \leq \Delta P_{NS}$), where ΔP_{NS} is the low (No Suction) threshold on ΔP. In addition, the pump flow signal is periodic with a large sinusoidal component.

2) Approaching Suction (AS): In this case, $\Delta P_{NS} < \Delta P \leq \Delta P_S$, where ΔP_S is the high (Suction) threshold on ΔP. That is, MPIP decreases much faster than MLVP causing ΔP to increase. The pump flow signal becomes less pulsatile comparing to the No Suction case.

3) Suction (S): During this event, the inlet cannula[1] is evidently obstructed, MPIP exhibits very large negative spikes, and MLVP is slightly less than zero (i.e., $\Delta P > \Delta P_S$). Furthermore, the pump flow waveform exhibits a sudden large drop in the slope of the envelope of the minimum pump flow signal instead of approximately having a sinusoidal form synchronized with heart rate.

In the following section, the time, frequency, and

This work was supported in part by NSF under Grant ECCS-0701365.

Y. Wang, G. Faragallah and M. A. Simaan are with the Department of Electrical Engineering and Computer Science, University of Central Florida, Orlando, FL 32816 USA (e-mail: wangyu810410@knights.ucf.edu; georgef@knights.ucf.edu; simaan@ucf.edu;).

E. Divo is with the School of Engineering Technology, Daytona State College, Daytona Beach, FL 32117 USA (e-mail: edivo@mail.ucf.edu).

[1] The cannula is a plastic rigid tube that connects the rotary pump to the left ventricle of the heart.

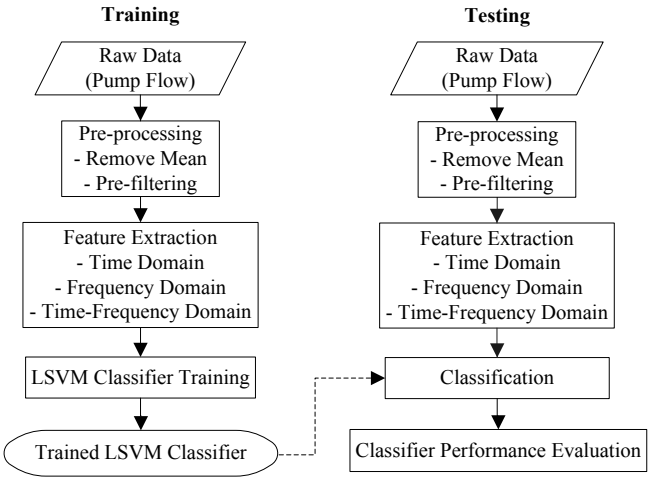

Fig. 1. Flow chart of the proposed suction detection algorithm.

time-frequency based suction indices extracted from the pump flow are described using a window of 5 seconds.

B. Feature Extraction

1) Time-based indices: The time index SI_1 is defined based on the mean, minimum, and maximum values of the pump flow [7]. The expression is as follows:

$$\mathrm{SI}_1 = \frac{2\times\mathrm{mean(PF)}-\mathrm{max(PF)}-\mathrm{min(PF)}}{\Delta \mathrm{e}} \tag{1}$$

where PF is pump flow signal and Δe is the peak-to-peak amplitude of PF. When suction is absent, the mean pump flow value is approximately half of the sum of the maximum and minimum values of pump flow, which shifts slightly towards minimum pump flow while approaching suction. When suction occurs, the mean pump flow value is close to the maximum pump flow value. Hence, SI_1 increases dramatically.

Time indices SI_2 and SI_3 are calculated with respect to the derivative of the pump flow signal as

$$\mathrm{SI}_2 = \frac{\left[\frac{\mathrm{d(PF)}}{\mathrm{dt}}\right]_{\max}}{\Delta \mathrm{e}} \tag{2}$$

$$\mathrm{SI}_3 = \frac{\left[\frac{\mathrm{d(PF)}}{\mathrm{dt}}\right]_{\min}}{\Delta \mathrm{e}} \tag{3}$$

where $\left[\frac{d(PF)}{dt}\right]_{max}$ is the maximum derivative of PF and $\left[\frac{d(PF)}{dt}\right]_{min}$ is the minimum derivative of PF, respectively. SI_2 increases obviously during suction, whereas SI_3 decreases at the beginning of suction.

2) Frequency-based indices: The frequency domain indices can detect the changes in the harmonic and subharnomic energy content of pump flow [3]. Consider $Q_P(\omega)$ as the Fourier transform of the pump flow signal and ω_0 as the fundamental frequency of pump flow. Also, consider $\omega_1 = \omega_0 - \omega_c$ and $\omega_2 = \omega_0 + \omega_c$, where ω_c is a threshold (in radians) that defines an interval centered at ω_0. The harmonic index SI_4 is defined as the ratio of the signal's total energy in the fundamental component frequency band to the total energy in the harmonic component frequency band, given by the expression

$$SI_4 = \frac{\int_{\omega_1}^{\omega_2}|Q_P(\omega)|d\omega}{\int_{\omega_2}^{\infty}|Q_P(\omega)|d\omega} \tag{4}$$

Another frequency index SI_5 is defined as the ratio of the subharmonic energy to the fundamental energy, given as

$$\mathrm{SI}_5 = \frac{\int_0^{\omega_1}|\mathrm{Q_P(\omega)}|\mathrm{d\omega}}{\int_{\omega_1}^{\omega_2}|\mathrm{Q_P(\omega)}|\mathrm{d\omega}} \tag{5}$$

When approaching suction, SI_4 starts to decrease and SI_5 starts to increase. In the case of suction event, SI_4 decreases and SI_5 increases abruptly due to the shift of energy from the fundamental band to both harmonic and subharmonic band, indicating the occurrence of suction.

3) Time-Frequency-based index: This method is used to supplement the frequency-domain approach [3]. The suction index SI_6 is defined as the standard deviation of instantaneous mean frequency of pump flow, expressed as

$$\mathrm{SI}_6 = \sqrt{\mathrm{var}\left(\langle\omega\rangle_{\mathrm{t}}^{\mathrm{SP}}\right)} \tag{6}$$

In (6), the instantaneous frequency is defined as the average frequency at a given time [8], expressed as

$$\langle\omega\rangle_{\mathrm{t}}^{\mathrm{SP}} = \frac{\int \omega \mathrm{P_{SP}(\omega,t)d\omega}}{\int \mathrm{P_{SP}(\omega,t)d\omega}} \tag{7}$$

where $P_{SP}(\omega, t)$ is the squared magnitude of the short-time Fourier transform (STFT). The value of SI_6 is small without suction and increases slightly when suction is approaching, and it increases abruptly during suction event.

The six indices described above are used as inputs to the LSVM classifier.

C. LSVM-based Suction Classifier

SVM is a reliable and powerful classification algorithm and has been successfully applied to various pattern recognition problems [9]. The main idea of SVM is to find the optimal separating hyperplane (with the maximum margin) between two classes (+1 or -1) of the data points.

LSVM is a very fast and simple algorithm, based on an implicit Lagrangian formulation of the dual of a simple reformulation of the standard quadratic problem of SVM [10]. Although LSVM is originally designed as a binary classifier, classification into additional classes is possible. In this work, a 2-step LSVM decision tree method is adopted for the 3-class problem. First, we separate the S case from the NS and AS cases since suction event is evidently different from NS and AS, and secondly NS and AS are classified by another LSVM. Details on the LSVM algorithm can be found in [10].

III. Result

Fig. 2 (a) shows a pump flow signal of a LVAD in vivo experiment used in [3]. The six suction indices derived from this signal are also plotted on the same figure. The changes in

these indices as the pump flow signal transitions from NS to AS to S are clearly evident in Fig. 2 (b)-(g). These indices are used as inputs to the LSVM classifier. The classifier is trained on a randomly selected set of 50% of the data and then tested on the remaining 50% of the data. The training and testing procedures and the description of the database of signals used are similar to those described in [3]. The two thresholds on ΔP used in the classifier, as mentioned in Section II, are chosen as $\Delta P_{NS} = 10$ mmHg and $\Delta P_S = 35$ mmHg. Due to the random selection of data samples, the classification is repeated 100 times. All experimental procedures are implemented using MATLAB[2].

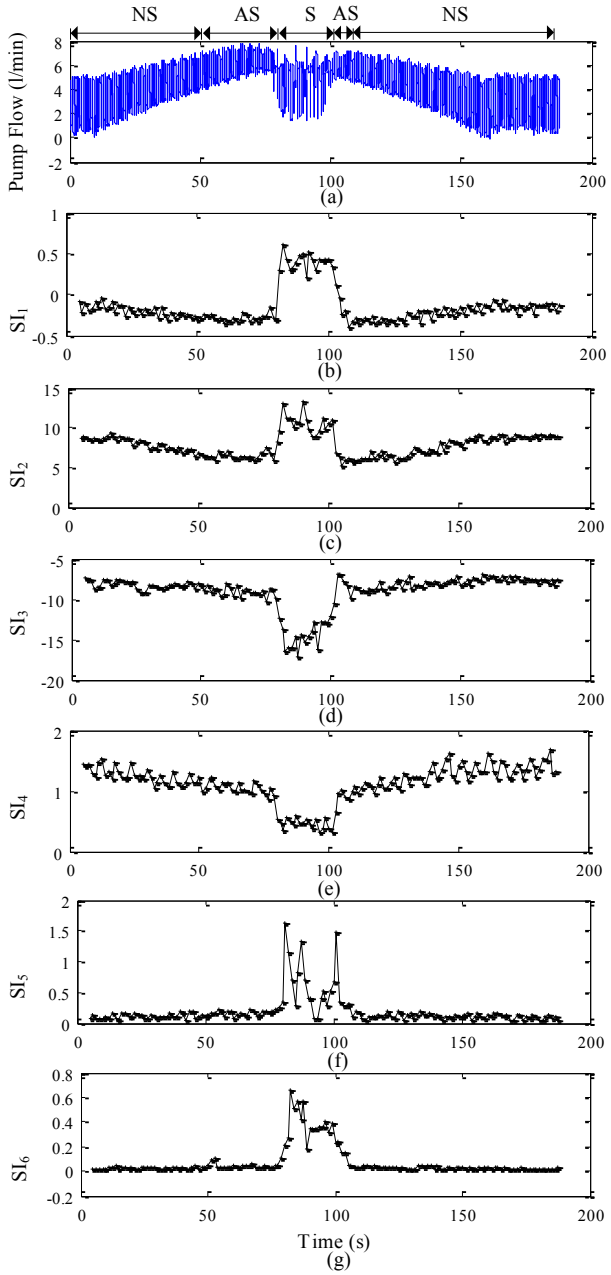

Fig. 2. Suction indices extracted from the pump flow. (a) Pump Flow. (b) SI_1. (c) SI_2. (d) SI_3. (e) SI_4. (f) SI_5. (g) SI_6.

[2] The MathWorks Inc., Natick, MA.

TABLE I
CLASSIFICATION RESULTS OF LSVM CLASSIFIER ON TEST SET[a]

	NS	AS	S	Total
NS	703.14 (92.89%)	53.36 (7.05%)	0.5 (0.06%)	757 (100%)
AS	37.33 (5.82%)	598.24 (93.33%)	5.43 (0.85%)	641 (100%)
S	0.09 (0.09%)	5.31 (5.31%)	94.6 (94.6%)	100 (100%)

[a]Actual classes are in rows, predicted in columns.

The average classification results of the proposed algorithm over 100 runs on the test set are shown in Table I. For NS, on average there are 53.36 samples misclassified as AS (7.05%) and only 0.5 samples are misclassified as S (0.06%). For AS, on average 37.33 samples are misclassified as NS (5.82%) and only 5.43 samples are incorrectly identified as S (0.85%). For S, on average the erroneous number of samples misclassified as NS and AS are as low as 0.09 (0.09%) and 5.31 (5.31%), respectively.

IV. DISCUSSION

A comparison study with three existing algorithms (CART [2], DA [3], and NN [4]) is conducted to evaluate the performance of the proposed method using the same database of signals and procedures described above. The performance evaluation criteria are: sensitivity (true positive rate), specificity (true negative rate), accuracy (the rate of the total number of predictions correctly classified) with their standard deviations, and the training/test time. Fig. 3 illustrates the comparison of the four approaches, showing that the LSVM-based algorithm occupies 7 of 9 performance indices (sensitivity, specificity, and accuracy of three cases, respectively) as highest classification accuracy and 4 of 9 smallest standard deviations (most stable performance). Note that the CART-based algorithm occupies 3 of 9 smallest standard deviations; however, there are 7 of 9 lowest classification accuracy indices for CART algorithm. The LSVM-based algorithm therefore has the advantage of high accuracy and stability when compared to other algorithms. In addition, the LSVM-based algorithm needs the least training time (learning speed) compared to the other three approaches as shown in Table II. This comparison is implemented on a 2-GHz Intel Pentium Dual CPU desktop computer with 3 gigabytes of memory.

The other two performance estimation criteria are the Receiver Operating Characteristic (ROC) curve and Area under ROC Curve (AUC). The ROC curve is a technique for visualizing, analyzing, and choosing classifiers based on their performance. The AUC is an index of the quantitative measure of the overall performance of the classifiers [11]. Note that in this paper, the ROC curve is not made for CART method due to the discrete characteristic of the CART classifier. In addition, since ROC curve is a graphical plot for a binary classifier algorithm, the ROC curves are

implemented only for the NS and AS cases since their characteristics is similar compared to the S case. Fig. 4 shows the ROC curves, indicating that the overall performance of the LSVM-based algorithm is better than that of NN and DA algorithms. Thus, in general, the LSVM-based approach appears to be superior to CART, DA, and NN algorithms in terms of classification performance.

Other more practical considerations in developing a suction detection algorithm are the computation and hardware in real time. For patients implanted with LVAD, suction must be identified in the order of seconds, and the six suction indices examined in this paper can be computed at a high rate (62.5 Hz), which means it can meet the LVAD requirements. Furthermore, with the current batch processors available, most conceivable features are able to be easily executed in real time. Therefore, the proposed system can be a valuable tool for real-time suction detection.

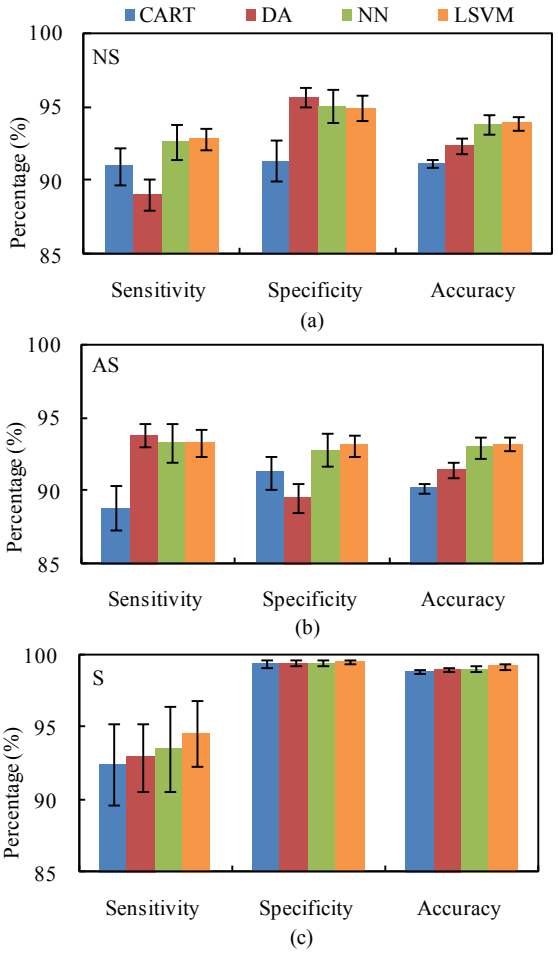

Fig. 3. Comparison of classification accuracy. (a) NS. (b) AS. (c) S. The brackets indicate the standard deviations.

TABLE II
COMPARISON OF AVERAGE TRAINING/TEST TIME ON 100 RUNS

	CART	DA	NN	LSVM
Training time (s)	0.534	0.248	3.126	0.063
Test time (s)	0.012	0.032	0.02	0.024

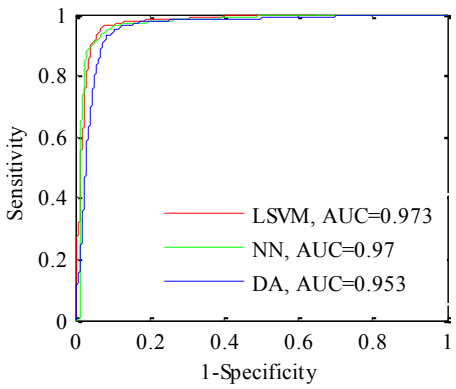

Fig. 4. Comparison of ROC curves between NS and AS cases.

V. CONCLUSION

In this study, an effective LSVM-based suction detection algorithm was presented. Six features were extracted from the pump flow signal and used as inputs to the algorithm. This algorithm combined with the decision tree strategy was used to implement a 3-group classification task. Compared to three existing approaches, the proposed algorithm showed effective accuracy with high stability and a short learning speed. Future work will focus on the development of a feedback control strategy to automatically adjust the pump speed in rotary LVADs to avoid the occurrence of suction, based on the proposed suction detection system.

REFERENCES

[1] M. Oshikawa, K. Araki, G. Endo, H. Anai, and M. Sato, "Sensorless controlling method for a continuous flow left ventricular assist device," *Artif. Organs*, vol. 24, no. 8, pp. 600-605, 2000.

[2] D. M. Karantonis, N. H. Lovell, P. J. Ayre, D. G. Mason, and S. L. Cloherty, "Identification and classification of physiologically significant pumping states in an implantable rotary blood pump," *Artif. Organs*, vol. 30, no. 9, pp. 671-679, 2006.

[3] A. Ferreira, S. Chen, M. A. Simaan, J. R. Boston, and J. F. Antaki, "A discriminant-analysis-based suction detection system for rotary blood pumps," in *Proc. 28th IEEE Annu. Int. Conf. Eng. Med. Biol.*, New York City, NY, 2006, pp. 5382–5385.

[4] D. M. Karantonis, S. L. Cloherty, N. H. Lovell, D. G. Mason, R. F. Salamonsen, and P. J. Ayre, "Noninvasive detection of suction in an implantable rotary blood pump using neural networks," *Int. J. Computation Intelligence and Appl.*, vol. 7, no. 3, pp. 237-247, 2008.

[5] L. Chisci, A. Mavino, G. Perferi, M. Sciandrone, C. Anile, G. Colicchio, and F. Fuggetta, "Real-time epileptic seizure prediction using AR models and support vector machines," *IEEE Trans. Biomed. Eng.*, vol. 57, no. 5, pp. 1124-1132, May 2010.

[6] S. R. I. Gabran, W. W. Moussa, M. M. A. Salama, and C. George, "Portable real-time support-vector-machine-based automated diagnosis and detection device of narcolepsy episodes," in *Proc. 31st IEEE Annu. Int. Conf. Eng. Med. Biol.*, Minneapolis, MN, 2009, pp. 903–906.

[7] M. Vollkron, H. Schima, L. Huber, R. Benkowski, G. Morello, and G. Wieselthaler, "Development of a suction detection system for axial blood pumps," *Artif. Organs*, vol. 28, no. 8, pp. 709-716, 2004.

[8] L. Cohen, *Time-Frequency Analysis*. Prentice-Hall, Englewood Cliffs, NJ, 1995.

[9] V. Vapnik, *Statistical Learning Theory*. New York: Wiley, 1998.

[10] O. L. Mangasarian and D. R. Musicant, "Lagrangian support vector machines," *J. Machine Learning Research*, vol. 1, pp. 161-177, 2001.

[11] T. Fawcett, "An introduction to ROC analysis," *Pattern Recognition Letters*, vol. 27, pp. 861-874, 2006.